

Article

# Simple Route to Synthesize Fully Conjugated Ladder Isomer Copolymers with Carbazole Units

Shuang Chen <sup>1</sup>, Feng Liu <sup>1,2,\*</sup>, Chao Wang <sup>1</sup>, Jinghui Shen <sup>1</sup> and Yonggang Wu <sup>1,\*</sup>

<sup>1</sup> College of Chemistry and Environmental Science, Hebei University, Baoding 071002, China; chengshuangfff@163.com (S.C.); WC19940119@163.com (C.W.); sjhui0218@163.com (J.S.)

<sup>2</sup> College of Physics Science and Technology, Hebei University, Baoding 071002, China

\* Correspondence: liufeng@hbu.edu.cn (F.L.); wuyonggang@hbu.edu.cn (Y.W.); Tel.: +86-158-3121-6174 (F.L.)

Received: 18 August 2019; Accepted: 2 October 2019; Published: 7 October 2019



**Abstract:** Two isomer polymers, P3 and P6, with fully conjugated ladder structures are presented by simple synthetic routes. The well-defined structures of fully conjugated ladder polymers P3 and P6 were ensured by the high yields of every reaction step. The fully rigid ladder structures were confirmed by nuclear magnetic resonance (NMR), fourier transform infrared spectroscopy (FTIR), and photophysical test. Polymers P3 and P6 with bulky alkyl side chains exhibit good solution processability and desirable thermostable properties. After the intramolecular cyclization reaction, the band gaps of polymers P3 and P6 become lower (2.86 eV and 2.66 eV, respectively) compared with polymers P1 and P4. This initial study provides insight for the rational design of fully ladder-conjugated isomeric polymers with well-defined structures.

**Keywords:** carbazole; ladder; BO embedded; isomer

## 1. Introduction

Fully conjugated ladder polymers (cLPs) have drawn extensive attention because of their rigid structure with  $\pi$ -conjugated systems [1–6]. The unique structure of cLPs confers favorable physical, optical, and chemical properties [7–10]. Thus, cLPs are promising candidates as organic materials [11–16], such as organic solar cells, organic thin film transistors, and organic light emitting diodes. However, there still exist some challenges to synthesize new cLPs with the desired solubility and fewer structure defects, and researchers have tried various methods to solve these difficulties [6,17–21], such as introducing bulky alkyl side chains to improve solubility, and introducing new reactive groups using new synthetic methods to synthesize ideal conjugated defect-free polymers.

Recently, researchers have introduced different heteroatoms [8,22–26], such as N, B, S, P, and Si, to the fused  $\pi$ -conjugated structure. This can effectively regulate the structure with desirable physical and chemical properties. The B-N unit, which has strong electron-withdrawing properties, can be used to construct new materials with good charge transport and photoconductivity in optoelectronic applications [22,27–34]. Hence, the integration of the B-N fragment into the fused  $\pi$ -conjugated ladder system may be a useful strategy to construct new cLPs. Wu's group [21,35–37] has conducted extensive work of this type. They once used the above strategy to synthesize a fused  $\pi$ -conjugated ladder compound and polymer [35]; the polymer exhibited good solution and thermal properties, with a UV-vis absorption peak at 455 nm; after the BN-embedded cyclization, the fused ladder-conjugated polymer presented a lower band gap.

In this work, we designed simple synthetic routes to synthesize two isomer polymers, P3 and P6, with BO-embedded fused  $\pi$ -conjugated ladder structure. The high yields of each synthesis step ensure the well-defined structure of the polymer with fewer structure defects. The BO-embedded fused  $\pi$ -conjugated ladder structures of P3 and P6 were confirmed by NMR, FTIR, and photophysical test.

Their thermal, photophysical, and electrochemical properties were also studied in detail. The main purpose of this paper is to provide an insight for synthesizing defect-free cLPs.

## 2. Materials and Methods

### 2.1. Materials

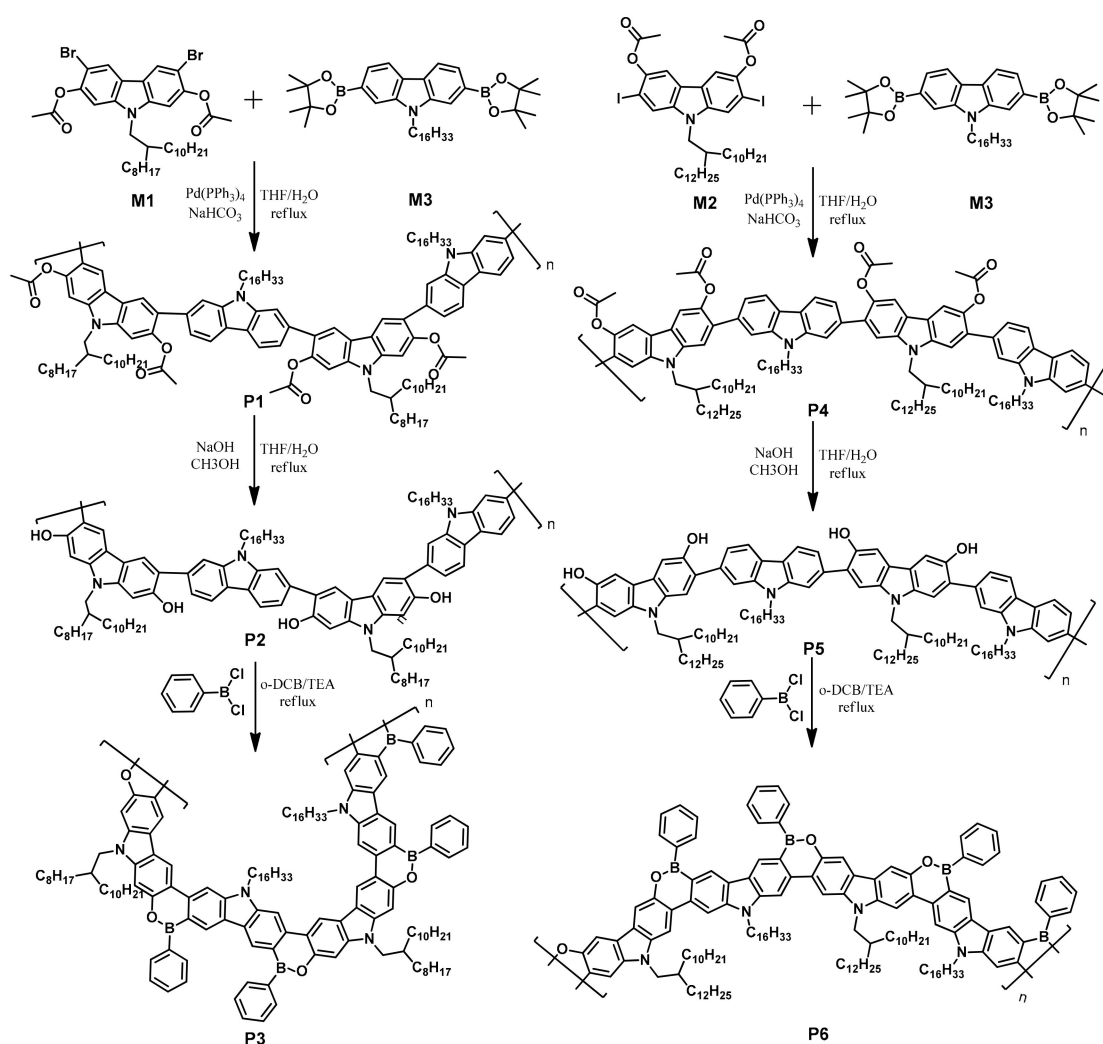
Commercial chemicals were used without further purification. Tetrahydrofuran (THF) and dichloromethane (DCM) were distilled by a standard process before use. All the reactions were monitored by thin layer chromatography (TLC) with silica gel 60 F254 (Merck, Germany, 0.2 mm).

### 2.2. Instrumentation

$^1\text{H}$  and  $^{13}\text{C}$  NMR data were obtained on a Bruker AV600 spectrometer. The electrochemical behavior was recorded by cyclic voltammetry (Holland, Ivium Plus II) with a standard three-electrode electrochemical cell, including a glassy carbon working electrode, a Pt wire counter electrode, and an  $\text{Ag}/\text{Ag}^+$  (0.01 M in  $\text{CH}_3\text{CN}$ ) reference electrode. The  $\text{CH}_2\text{Cl}_2$  solution contains 0.1 M tetrabutylammonium hexafluorophosphate (TBAPF6). The scan range was  $-1.4$ – $1.7$  V, and the scan rate was  $50 \text{ mV}\cdot\text{s}^{-1}$ . UV-visible absorption spectra were obtained on a Shimadzu UV-visible spectrometer model UV-2550 (Japan). Fluorescence spectra were obtained by a Shimadzu RF-5301PC fluorescence spectrophotometer (Japan). MALDI-TOF analyses were acquired with Bruker Daltonics Inc Autoflex III (US). Thermal gravimetric analysis (TGA) and differential scanning calorimetry (DSC) measurements were carried out on Perkin-Elmer Pyris 6 TGA (US) ( $10 \text{ }^\circ\text{C}/\text{min}$ ,  $\text{N}_2$ ) and Perkin-Elmer Diamond DSC instruments (US) ( $10 \text{ }^\circ\text{C}/\text{min}$ ,  $\text{N}_2$ ), respectively, to record TGA and DSC curves.

### 2.3. General Synthesis of Conjugated Ladder Polymers P3 and P6

The conjugated ladder-type copolymers were synthesized in three steps (Scheme 1). First, polymers P1 and P4 were synthesized by using Suzuki coupling conditions and  $\text{Pd}(\text{PPh}_3)_4$  as a catalyst. Then, the ester group was converted into a hydroxy group. Last, phenylboron dichloride was added for the intramolecular cyclization reaction to give polymers P3 and P6. The detail synthesis for the reaction monomers, compounds, and polymers is provided as supporting information.

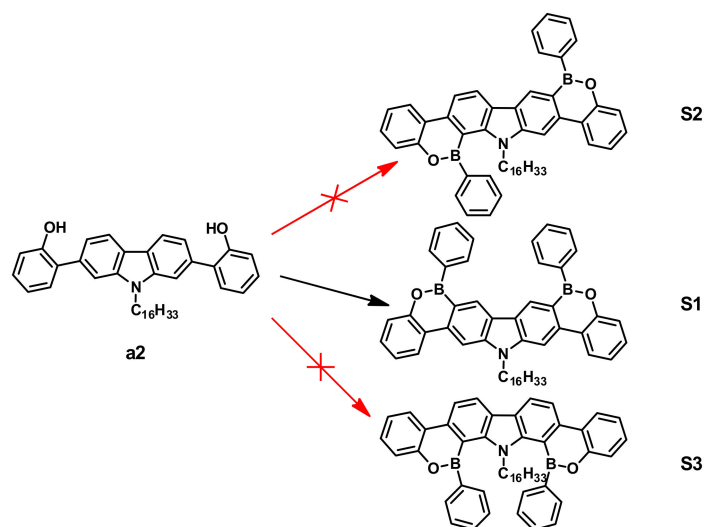


**Scheme 1.** Synthetic routes to polymer sP3 and P6.

### 3. Results

#### 3.1. Synthetic Route Discussion

To ensure the synthetic route could successfully synthesize the defect-free fully  $\pi$ -conjugated ladder polymers, we first used model compounds to explore the synthetic routes. The compound S1 was synthesized in high yields above 96%. As seen in Scheme 2, the carbazole and phenol units of compound a2 were linked by a single bond; thus, the phenol-carbazole bond unit can have free rotation. The intramolecular cyclization may form three possible isomers including compounds S1, S2, and S3. However, the structure of the product was identified by NMR spectrum, MALDI-TOF, and FTIR (see supporting information), and only one product, compound S1, was observed. The geometry optimizations of compound S1, S2, and S3 were managed within the framework of density functional theory (DFT) using B3LYP functional at the level of 6-31G(d) (Figure 1). Methyl units were used to replace branched side chains. The electronic and thermal free energies (E) of compound S1, S2, and S3 were  $-1679.65$  KJ/mol,  $-1679.64$  KJ/mol, and  $-1679.63$  KJ/mol, respectively. The compound S1 had the lowest electronic and thermal free energies, indicating that S1 is more stable than S2 and S3 [38–41]. The high yield of the intramolecular cyclization reaction and deterministic structure indicates a high feasibility to synthesize the fully conjugated ladder polymers P3 and P6. The photophysical and electrochemical properties of the compounds were also studied (see supporting information).



Scheme 2. Synthetic route to compound S1.

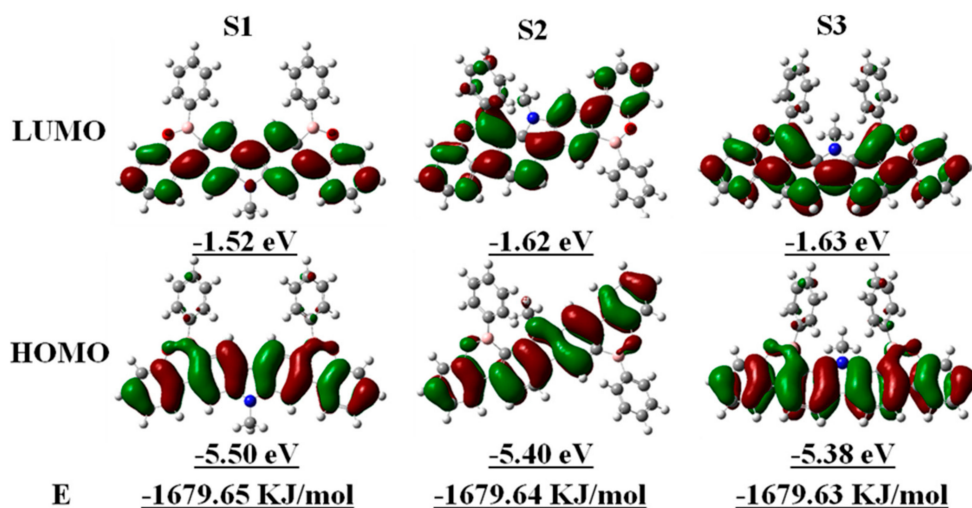


Figure 1. Optimal structure and total energy of compounds S1, S2, and S3 based on B3LYP/6-31G(d) level by Gaussian 16.

### 3.2. NMR Spectra of Polymers

The structures of the polymers were first identified by NMR (Figure 2). First, both the NMR spectra of P1 and P4 showed a clear peak around 2.44 ppm. This peak was assigned to the  $-\text{COOCH}_3$  protons. Then, when the ester group was converted into the hydroxy group, the peak around 2.44 ppm disappeared completely, and a new peak appeared around 5.30 ppm or 5.67 ppm. This new peak was assigned to the  $-\text{OH}$  proton. Last, after the intramolecular cyclization reaction, the peak around 5.30 ppm or 5.67 ppm completely disappeared, and a new peak appeared around 9.10 ppm. This new peak may be assigned to the protons of the benzene ring. Comparing the NMR spectra of P1, P2, P3, P4, P5, and P6, the completely disappeared peaks and newly formed peaks indicate that each step of the synthetic reaction has a high yield, and the structures of P3 and P6 have a well-defined structure with fewer defects.

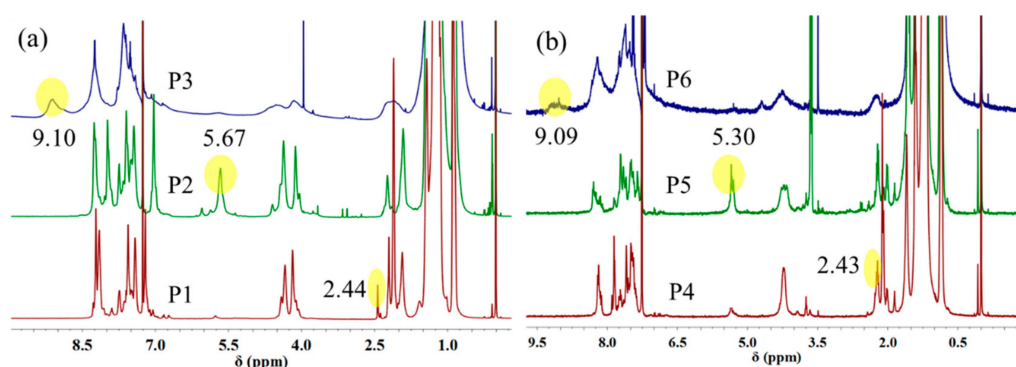


Figure 2. NMR spectra of polymers recorded in  $\text{CDCl}_3$ .

### 3.3. Size-Exclusion Chromatography (SEC) Trace for Polymers

The molecular weight of polymers was investigated by size-exclusion chromatography (SEC) in THF (polystyrene as standard) (Figure 3), and the data are listed in Table 1. The  $M_n$  values of P1, P3, P4, and P6 were  $7.1 \times 10^3$  g/mol,  $7.8 \times 10^3$  g/mol,  $9.8 \times 10^3$  g/mol, and  $10.8 \times 10^3$  g/mol, respectively, and the polydispersity index ( $D$ ) was 1.49, 1.46, 1.59, and 1.40, respectively. The  $M_n$  values of P3 and P6 can be recognized as being overestimated relative to the actual molecular weight due to the rigid structure. The planar structure of the polymers can increase the hydrodynamic radius in solution.

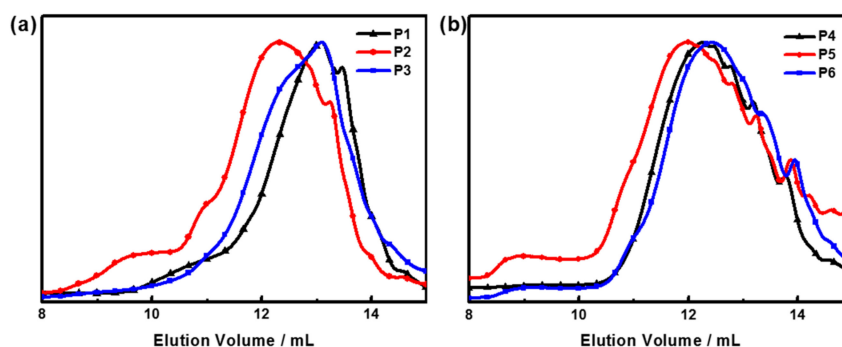


Figure 3. Size-exclusion chromatography (SEC) chromatograms of polymers.

Table 1. Polymer Properties and Yields.

	$M_n \times 10^3$ g/mol <sup>a</sup>	$M_w \times 10^3$ g/mol <sup>a</sup>	$D$ <sup>a</sup>	$T_{5\%}/^\circ\text{C}$ <sup>b</sup>	HOMO/eV <sup>c</sup>	LUMO/eV <sup>d</sup>	$E_{\text{gap}}$ /eV <sup>e</sup>
P1	7.1	10.6	1.49	381	−5.52	−2.38	3.14
P3	7.8	11.4	1.46	363	−5.62	−2.76	2.86
P4	9.8	15.6	1.59	351	−5.56	−2.60	3.00
P6	10.8	15.1	1.40	368	−5.68	−3.02	2.66

<sup>a</sup>  $D = M_w/M_n$ . Determined by SEC. <sup>b</sup> Determined by thermogravimetric analysis (TGA),  $T_{5\%}$  was the temperature for 5% weight loss. <sup>c</sup> Measured by cyclic voltammetry (CV),  $E_{\text{HOMO}} = -(E_{\text{ox}} + 4.8)$  eV. <sup>d</sup> Calculated by  $E_{\text{LUMO}} = E_{\text{HOMO}} + E_{\text{gap}}$ . <sup>e</sup> Band gap calculated from the onset of the absorption in the UV-vis spectra,  $E_{\text{gap}} = 1240/\lambda$ .

Usually, the fully  $\pi$ -conjugated ladder polymers showed limited solubility due to the rigid structure and strong intramolecular interactions. To solve this problem, bulky alkyl chains were introduced into the polymer structures. Due to the bulky alkyl chains, polymers P3 and P6 showed good solubility in common organic solvents such as chloroform, THF, and *N,N*-dimethylformamide (DMF).

### 3.4. Thermal Properties of Polymers

The thermal properties of copolymers were evaluated by thermal gravimetric analysis (TGA) (Figure 4) and differential scanning calorimetry (DSC) (Figure 5). The decomposition temperatures (with a 5% mass loss) for polymers P1, P3, P4, and P6 were 381 °C, 363 °C, 351 °C, and 368 °C,

respectively. In the heating and cooling DSC scans, there were no apparent glass transition processes or other thermal processes. This phenomenon suggested that the polymers have an amorphous structure. Also, their thermal properties were not influenced by the isomeric effect.

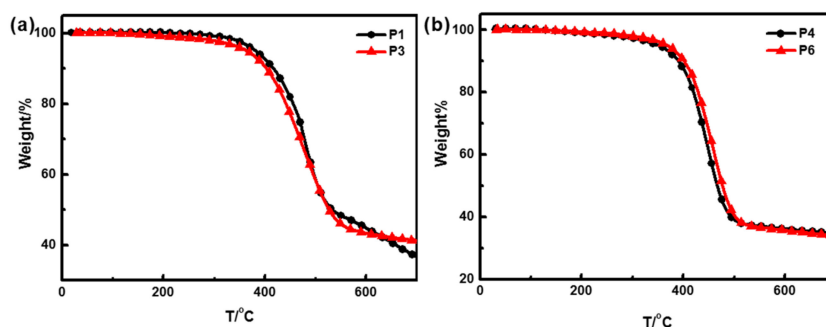


Figure 4. TGA traces of polymer.

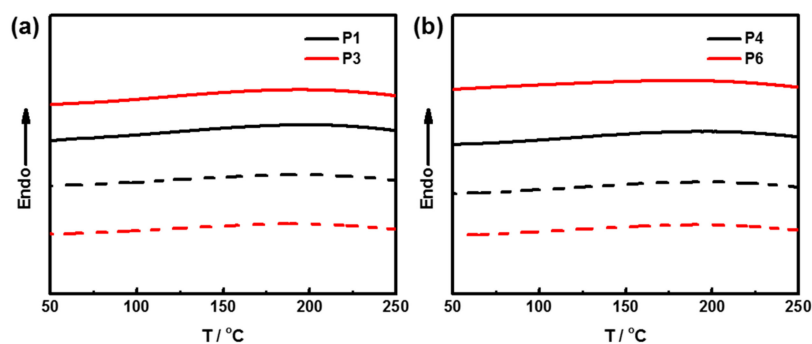


Figure 5. Differential scanning calorimetry (DSC) thermograms of polymers (solid lines indicate the heating DSC scan, and dash lines indicate cooling DSC scan).

### 3.5. FTIR Spectra of Polymers

Furthermore, the intramolecular cyclization reaction was also confirmed by FTIR spectrum (Figure 6). First, the polymers P1 and P4 showed a  $\text{-C=O}$  stretch peak (around  $1736\text{ cm}^{-1}$ ). After the dehydration reaction, the ester group changed into a hydroxyl group, with the loss of the  $\text{-C=O}$  stretch peak and a new  $\text{-OH}$  stretch peak ( $3542\text{ cm}^{-1}$  for polymer P2,  $3455\text{ cm}^{-1}$  for polymer P4). The  $\text{-C=O}$  stretch peak completely disappeared, which indicates the high yield of the dehydration reaction. Last, comparing polymer P2 with P3, and P4 with P6, the  $\text{-OH}$  stretch peak completely disappeared, indicating the high yield of the intramolecular cyclization reaction and the less structure-defect for polymers P3 and P6.

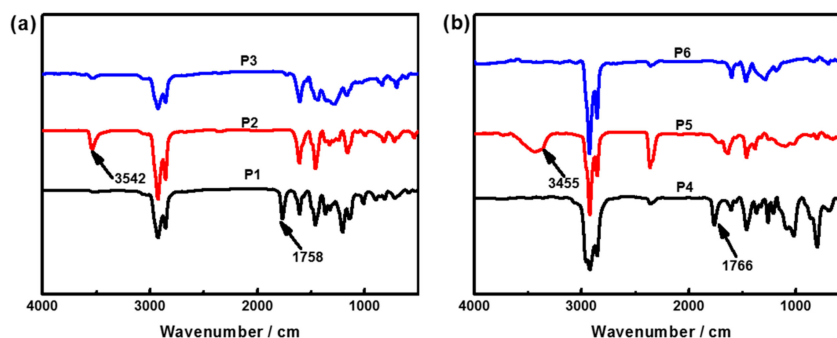
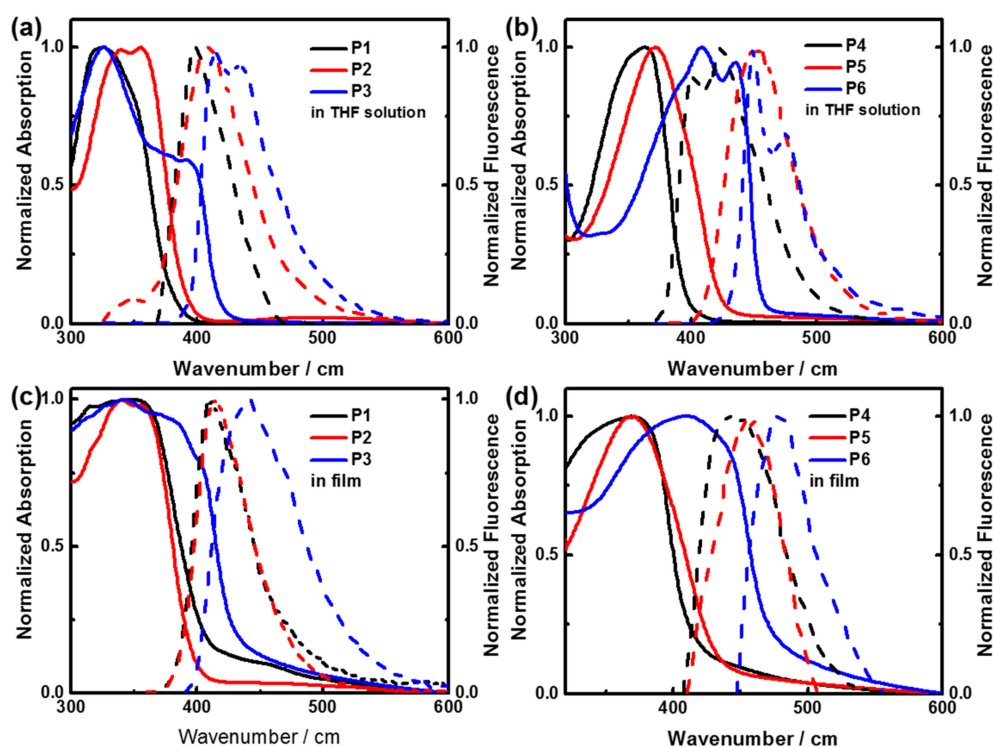


Figure 6. FTIR spectra of polymers before and after intramolecular cyclization reaction.

### 3.6. Photophysical Properties of Polymers

The UV-vis absorption and fluorescence spectra of polymers were measured in a diluted THF solution (Figure 7a,b). Polymers P1, P2, and P3 showed a similar UV-vis absorption peak around 330 nm (326 nm, 344 nm, and 326 nm, respectively). Clearly, the polymer P3 showed another UV-vis absorption peak around 390 nm, which is attributed to the extended  $\pi$ -conjugated structure after the B-O intramolecular cyclization reaction. The polymers P1, P2, and P3 exhibited maximum emission peaks at 398 nm, 409 nm, and 435 nm, respectively. The quantum yields ( $\Phi_f$ ) of P1 and P3 were calculated as 0.66 and 0.96, respectively, with 9,10-diphenylanthracene ( $\Phi_f = 0.95$ ) as the reference. The higher  $\Phi_f$  value of P3 can be ascribed to the more rigid structure and electron-donor properties when phenyl groups are introduced. The UV-vis absorption and fluorescence spectra of polymers in film were also measured. The UV-vis absorption peaks of polymers P1, P2, and P3 were around 337 nm, 342 nm, and 345 nm, respectively. Compared with the UV-vis absorption of polymers in THF solution, the UV-vis absorption of polymers in film did not show any shifts. Meanwhile, the emission peaks of polymers in film showed a small red shift compared with the emission peaks of polymers in THF solution.



**Figure 7.** (a) Photophysical properties of polymers P1, P2, and P3 in tetrahydrofuran (THF) solution. (b) Photophysical properties of polymers P4, P5, and P6 in THF solution. (c) Photophysical properties of polymers P1, P2, and P3 in film. (d) Photophysical properties of polymers P4, P5, and P6 in film. The solid lines represent UV-vis absorption spectra. The dash lines indicate fluorescence emission spectra.

Polymers P4 and P5 showed a single UV-vis absorption peak around 363 nm and 372 nm in THF solution, respectively. Polymer P6 showed two UV-vis absorption peaks around 380 nm and 435 nm, respectively. Compared with P4, the UV-vis absorption peak of P6 showed an obvious red shift. The polymers P4, P5, and P6 exhibited maximum emission peaks at 424 nm, 450 nm, and 476 nm, respectively. The quantum yields ( $\Phi_f$ ) of P4 and P6 were calculated as 0.72 and 0.98, respectively, with 9,10-diphenylanthracene ( $\Phi_f = 0.95$ ) as the reference. Meanwhile, compared with the UV-vis absorption and emission of polymers in THF solution, the UV-vis absorption and emission of polymers in film showed a small red shift.

Compared with P3, the UV-vis absorption peaks of P6 in THF solution showed an obvious red shift, as the structure of P6 may show more rigid planar structures. The band gap of polymers P1, P3, P4, and P6 were 3.14 eV, 2.86 eV, 3.00 eV, and 2.66 eV, respectively. Compared with P1 and P4, P3 and P6 showed a lower band gap.

### 3.7. Electrochemical Properties of Polymers

The electrochemical properties of polymers were assessed using cyclic voltammetry and the Fc/Fc<sup>+</sup> redox system as the internal standard (−4.80 eV). The cyclic voltammogram (CV) measurements are summarized in Figure 8 and Figure S4. All the data of polymers are list in Table 1 and Table S1. The HOMO values of polymers P1, P3, P4, and P6 were −5.52 eV, −5.62 eV, −5.56 eV, and −5.68 eV, respectively. The LUMO values of polymers P1, P3, P4, and P6 were −2.38 eV, −2.76 eV, −2.60 eV, and −3.02 eV, respectively.

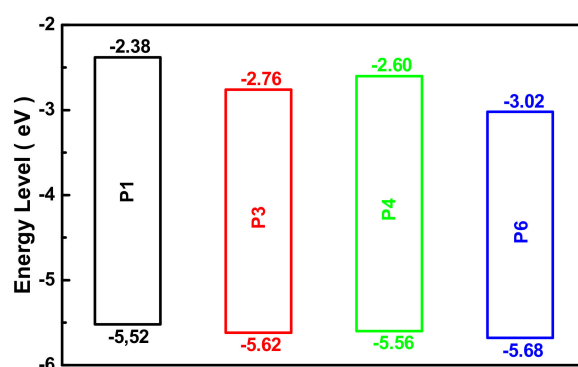


Figure 8. Cyclic voltammograms of polymers.

## 4. Conclusions

Two isomer polymers P3 and P6 with fully conjugated ladder structures have been presented. Simple synthetic routes with a high reaction yield ensure the well-defined structures of fully conjugated ladder polymers P3 and P6 with fewer structure defects. The rigid structures were confirmed by NMR, FTIR, and photophysical test. Polymers P3 and P6 exhibited good solution processability. The  $M_n$  values were  $7.8 \times 10^3$  g/mol and  $10.8 \times 10^3$  g/mol for P3 and P6, respectively. The polymers P3 and P6 showed two distinct UV-vis absorption bands. The HOMO values were −5.62 eV and −5.68 eV for P3 and P6, respectively. Compared with P1 and P4, P3 and P6 showed a lower band gap (2.86 eV and 2.66 eV, respectively). The TGA result showed that all the polymers had desirable thermostable properties. This initial study provides insight for the rational design of fully ladder-conjugated isomeric polymers with well-defined structures.

**Supplementary Materials:** The following are available online at <http://www.mdpi.com/2073-4360/11/10/1619/s1>: Optical properties of products, <sup>1</sup>H and <sup>13</sup>C NMR, and FTIR spectra. Figure S1: Cyclic voltammograms of compounds. Table S1: CV data of compounds.

**Author Contributions:** All authors designed and contributed to this study. S.C. executed the experiment and wrote the paper. F.L. and Y.W. edited the paper and gave final approval of the version to be submitted. All authors participated in the discussion and commented on the paper.

**Funding:** This work was supported by the Outstanding Doctoral Cultivation Project of Hebei University (YB201501), and the Natural Science Foundation of Hebei Province (B2019201337).

**Conflicts of Interest:** The authors declare no conflict of interest.

## References

1. Trilling, F.; Ausländer, M.-K.; Scherf, U. Ladder-Type Polymers and Ladder-Type Polyelectrolytes with On-Chain Dibenz [a,h] anthracene Chromophores. *Macromolecules* **2019**, *52*, 3115–3122. [[CrossRef](#)]

2. Takagi, K.; Tanaka, H.; Mikami, K. Ladderization of polystyrene derivatives by palladium-catalyzed polymer direct arylation. *Polym. Chem.* **2019**, *10*, 2647–2652. [[CrossRef](#)]
3. Zhu, C.; Kalin, A.J.; Fang, L. Covalent and Noncovalent Approaches to Rigid Coplanar  $\pi$ -Conjugated Molecules and Macromolecules. *Acc. Chem. Res.* **2019**, *52*, 1089–1100. [[CrossRef](#)] [[PubMed](#)]
4. Yu, L.; Chen, M.; Dalton, L.R. Ladder polymers: Recent developments in syntheses, characterization, and potential applications as electronic and optical materials. *Chem. Mater.* **1990**, *2*, 649–659. [[CrossRef](#)]
5. Teo, Y.C.; Lai, H.W.; Xia, Y. Synthesis of Ladder Polymers: Developments, Challenges, and Opportunities. *Chem. A Eur. J.* **2017**, *23*, 14101–14112. [[CrossRef](#)]
6. Congzhi, Z.; Lei, F. Locking the Coplanar Conformation of  $\pi$ -Conjugated Molecules and Macromolecules Using Dynamic Noncovalent Bonds. *Macromol. Rapid Commun.* **2018**, *39*, 1700241. [[CrossRef](#)]
7. Ren, Y.; Baumgartner, T. Ladder-Type  $\pi$ -Conjugated 4-Hetero-1,4-dihydrophosphinines: A Structure–Property Study. *Chem. A Eur. J.* **2010**, *5*, 1918–1929. [[CrossRef](#)]
8. Zheng, T.; Cai, Z.; Ho, W.R.; Yau, S.H.; Sharapov, V.; Goodson, I.T.; Yu, L. Synthesis of Ladder-Type Thienoacenes and Their Electronic and Optical Properties. *J. Am. Chem. Soc.* **2016**, *138*, 868–875. [[CrossRef](#)]
9. Alahmadi, A.F.; Lalancette, R.A.; Jäkle, F. Highly Luminescent Ladderized Fluorene Copolymers Based on B–N Lewis Pair Functionalization. *Macromol. Rapid Commun.* **2018**, *39*, 1800456. [[CrossRef](#)]
10. Liu, F.; Wu, Y.; Wang, C.; Ma, J.; Wu, F.; Zhang, Y.; Ba, X. Synthesis and Characterization of Fully Conjugated Ladder Naphthalene Bisimide Copolymers. *Polymers* **2018**, *10*, 790. [[CrossRef](#)]
11. Wu, Y.; Zhang, J.; Fei, Z.; Bo, Z. Spiro-bridged ladder-type poly(p-phenylene)s: Towards structurally perfect light-emitting materials. *J. Am. Chem. Soc.* **2008**, *130*, 7192–7193. [[CrossRef](#)] [[PubMed](#)]
12. Babel, A.; Jenekhe, S.A. High Electron Mobility in Ladder Polymer Field-Effect Transistors. *J. Am. Chem. Soc.* **2003**, *125*, 13656–13657. [[CrossRef](#)] [[PubMed](#)]
13. Durban, M.M.; Kazarinoff, P.D.; Segawa, Y.; Luscombe, C.K. Synthesis and Characterization of Solution-Processable Ladderized n-Type Naphthalene Bisimide Copolymers for OFET Applications. *Macromolecules* **2011**, *44*, 4721–4728. [[CrossRef](#)]
14. Cai, Z.; Awais, M.A.; Zhang, N.; Yu, L. Exploration of Syntheses and Functions of Higher Ladder-type  $\pi$ -Conjugated Heteroacenes. *Chem* **2018**, *4*, 2538–2570. [[CrossRef](#)]
15. Sun, H.; Vagin, M.; Wang, S.; Crispin, X.; Forchheimer, R.; Berggren, M.; Fabiano, S. Complementary Logic Circuits Based on High-Performance n-Type Organic Electrochemical Transistors. *Adv. Mater.* **2018**, *30*, 1704916. [[CrossRef](#)] [[PubMed](#)]
16. Wang, Y.; Guo, H.; Harbuzaru, A.; Uddin, M.A.; Arrechea-Marcos, I.; Ling, S.; Yu, J.; Tang, Y.; Sun, H.; López Navarrete, J.T.; et al. (Semi)ladder-Type Bithiophene Imide-Based All-Acceptor Semiconductors: Synthesis, Structure–Property Correlations, and Unipolar n-Type Transistor Performance. *J. Am. Chem. Soc.* **2018**, *140*, 6095–6108. [[CrossRef](#)] [[PubMed](#)]
17. Lee, J.; Rajeeva, B.B.; Yuan, T.; Guo, Z.-H.; Lin, Y.-H.; Al-Hashimi, M.; Zheng, Y.; Fang, L. Thermodynamic synthesis of solution processable ladder polymers. *Chem. Sci.* **2016**, *7*, 881–889. [[CrossRef](#)]
18. Zeng, W.; Gopalakrishna, T.Y.; Phan, H.; Tanaka, T.; Heng, T.S.; Ding, J.; Osuka, A.; Wu, J. Superoctazethrene: An Open-Shell Graphene-like Molecule Possessing Large Diradical Character but Still with Reasonable Stability. *J. Am. Chem. Soc.* **2018**, *140*, 14054–14058. [[CrossRef](#)] [[PubMed](#)]
19. Matsuoka, W.; Ito, H.; Itami, K. Rapid Access to Nanographenes and Fused Heteroaromatics by Palladium-Catalyzed Annulative  $\pi$ -Extension Reaction of Unfunctionalized Aromatics with Diiodobiaryls. *Angew. Chem. Int. Ed.* **2017**, *129*, 12392–12396. [[CrossRef](#)]
20. Koga, Y.; Kaneda, T.; Saito, Y.; Murakami, K.; Itami, K. Synthesis of partially and fully fused polyaromatics by annulative chlorophenylene dimerization. *Science* **2018**, *359*, 435–439. [[CrossRef](#)] [[PubMed](#)]
21. Ren, X.; Zhang, H.; Song, M.; Cheng, C.; Zhao, H.; Wu, Y. One-Step Route to Ladder-Type C–N Linked Conjugated Polymers. *Macromol. Chem. Phys.* **2019**, *220*, 1900044. [[CrossRef](#)]
22. Curiel, D.; Más-Montoya, M.; Usea, L.; Espinosa, A.; Orenes, R.A.; Molina, P. Indolocarbazole-based ligands for ladder-type four-coordinate boron complexes. *Org. Lett.* **2012**, *14*, 3360–3363. [[CrossRef](#)] [[PubMed](#)]
23. Wakim, S.; Bouchard, J.; Blouin, N.; Michaud, A.; Leclerc, M. Synthesis of Diindolocarbazoles by Ullmann Reaction: A Rapid Route to Ladder Oligo(p-aniline)s. *Org. Lett.* **2004**, *6*, 3413–3416. [[CrossRef](#)] [[PubMed](#)]
24. Fukazawa, A.; Yamada, H.; Yamaguchi, S. Phosphonium- and borate-bridged zwitterionic ladder stilbene and its extended analogues. *Angew. Chem. Int. Ed.* **2008**, *47*, 5582–5585. [[CrossRef](#)] [[PubMed](#)]

25. Matsuda, T.; Kadowaki, S.; Goya, T.; Murakami, M. Synthesis of Silafluorenes by Iridium-Catalyzed [2 + 2 + 2] Cycloaddition of Silicon-Bridged Diynes with Alkynes. *Org. Lett.* **2007**, *9*, 133–136. [[CrossRef](#)]
26. Zhu, C.; Ji, X.; You, D.; Chen, T.L.; Mu, A.U.; Barker, K.P.; Klivansky, L.M.; Liu, Y.; Fang, L. Extraordinary Redox Activities in Ladder-Type Conjugated Molecules Enabled by B←N Coordination-Promoted Delocalization and Hyperconjugation. *J. Am. Chem. Soc.* **2018**, *140*, 18173–18182. [[CrossRef](#)] [[PubMed](#)]
27. Tasior, M.; Gryko, D.T. Synthesis and Properties of Ladder-Type BN-Heteroacenes and Diazabenzoindoles Built on a Pyrrolopyrrole Scaffold. *J. Org. Chem.* **2016**, *81*, 6580–6586. [[CrossRef](#)]
28. Pais, V.F.; Alcaide, M.M.; López-Rodríguez, R.; Collado, D.; Nájera, F.; Pérez-Inestrosa, E.; Álvarez, E.; Lassaletta, J.M.; Fernández, R.; Ros, A. Strongly Emissive and Photostable Four-Coordinate Organoboron N,C Chelates and Their Use in Fluorescence Microscopy. *Chem. A Eur. J.* **2015**, *21*, 15369–15376. [[CrossRef](#)]
29. Bosdet, M.J.D.; Jaska, C.A.; Piers, W.E.; And, T.S.S.; Parvez, M. Blue Fluorescent 4a-Aza-4b-boraphenanthrenes. *Chem. A Eur. J.* **2007**, *9*, 1395–1398. [[CrossRef](#)]
30. Long, X.; Ding, Z.; Dou, C.; Zhang, J.; Liu, J.; Wang, L. Polymer Acceptor Based on Double B←N Bridged Bipyridine (BNBP) Unit for High-Efficiency All-Polymer Solar Cells. *Adv. Mater.* **2016**, *28*, 6504–6508. [[CrossRef](#)]
31. Zhu, C.; Guo, Z.-H.; Mu, A.U.; Liu, Y.; Wheeler, S.E.; Fang, L. Low Band Gap Coplanar Conjugated Molecules Featuring Dynamic Intramolecular Lewis Acid–Base Coordination. *J. Org. Chem.* **2016**, *81*, 4347–4352. [[CrossRef](#)] [[PubMed](#)]
32. Pais, V.F.; Ramírezlópez, P.; Romeroarenas, A.; Collado, D.; Nájera, F.; Pérez-Inestrosa, E.; Fernández, R.; Lassaletta, J.M.; Ros, A.; Pischel, U. Red-Emitting Tetracoordinate Organoboron Chelates: Synthesis, Photophysical Properties, and Fluorescence Microscopy. *J. Org. Chem.* **2016**, *81*, 9605–9611. [[CrossRef](#)] [[PubMed](#)]
33. Shimogawa, H.; Yoshikawa, O.; Aramaki, Y.; Murata, M.; Wakamiya, A.; Murata, Y. 4,7-Bis[3-(dimesitylboryl)thien-2-yl] benzothiadiazole: Solvato-, Thermo-, and Mechanochromism Based on the Reversible Formation of an Intramolecular B-N Bond. *Chem. A Eur. J.* **2017**, *23*, 3784–3791. [[CrossRef](#)] [[PubMed](#)]
34. Wang, X.; Zhang, F.; Liu, J.; Tang, R.; Fu, Y.; Wu, D.; Xu, Q.; Zhuang, X.; He, G.; Feng, X. Ladder-Type BN-Embedded Heteroacenes with Blue Emission. *Org. Lett.* **2013**, *15*, 5714–5717. [[CrossRef](#)] [[PubMed](#)]
35. Liu, F.; Zhang, H.; Dong, J.; Wu, Y.; Li, W. Highly Efficient Synthesis of a Ladder-Type BN-Heteroacene and Polyheteroacene. *Asian J. Org. Chem.* **2018**, *7*, 465–470. [[CrossRef](#)]
36. Shen, X.; Wu, Y.; Bai, L.; Zhao, H.; Ba, X. Microwave-assisted synthesis of 4,9-linked pyrene-based ladder conjugated polymers. *J. Polym. Sci. Part A Polym. Chem.* **2017**, *55*, 1285–1288. [[CrossRef](#)]
37. Cheng, J.; Li, B.; Ren, X.; Liu, F.; Zhao, H.; Wang, H.; Wu, Y.; Chen, W.; Ba, X. Highly twisted ladder-type backbone bearing perylene diimides for non-fullerene acceptors in organic solar cells. *Dye. Pigment.* **2019**, *161*, 221–226. [[CrossRef](#)]
38. Kakkar, R.; Pathak, M.; Radhika, N.P. A DFT study of the structures of pyruvic acid isomers and their decarboxylation. *Org. Biomol. Chem.* **2006**, *4*, 886–895. [[CrossRef](#)]
39. Ghiasi, R.; Ara, T.J.; Hakimyoun, A.H. Spectroscopic studies and molecular orbital analysis on platinanaphthalenes and ring-fused B-N platinanaphthalenes. *Russ. J. Phys. Chem. A* **2014**, *88*, 616–624. [[CrossRef](#)]
40. Türker, L. A DFT study on TNGU isomers and aluminized cis-TNGU composites. *Def. Technol.* **2018**, *14*, 109–118. [[CrossRef](#)]
41. Liu, D.; Yu, B.; Su, X.; Wang, X.; Zhang, Y.-M.; Li, M.; Zhang, S.X.-A. Photo-/Baso-Chromisms and the Application of a Dual-Addressable Molecular Switch. *Chem. Asian J.* **2019**, *14*, 2838–2845. [[CrossRef](#)] [[PubMed](#)]

